



This is a repository copy of *Supraglacial ponds regulate runoff from Himalayan debris-covered glaciers*.

White Rose Research Online URL for this paper:

<https://eprints.whiterose.ac.uk/124614/>

Version: Accepted Version

Article:

Irvine-Fynn, T., Porter, P.R., Rowan, A.V. orcid.org/0000-0002-3715-5554 et al. (6 more authors) (2017) Supraglacial ponds regulate runoff from Himalayan debris-covered glaciers. *Geophysical Research Letters*, 44 (33). 11,894-11,904. ISSN 0094-8276

<https://doi.org/10.1002/2017GL075398>

Reuse

Items deposited in White Rose Research Online are protected by copyright, with all rights reserved unless indicated otherwise. They may be downloaded and/or printed for private study, or other acts as permitted by national copyright laws. The publisher or other rights holders may allow further reproduction and re-use of the full text version. This is indicated by the licence information on the White Rose Research Online record for the item.

Takedown

If you consider content in White Rose Research Online to be in breach of UK law, please notify us by emailing eprints@whiterose.ac.uk including the URL of the record and the reason for the withdrawal request.



eprints@whiterose.ac.uk
<https://eprints.whiterose.ac.uk/>

Supraglacial ponds regulate runoff from Himalayan debris-covered glaciers

**Tristram D.L. Irvine-Fynn^{1*}, Philip R. Porter², Ann V. Rowan³, Duncan J. Quincey⁴,
Morgan J. Gibson¹, Jonathan W. Bridge⁵, C. Scott Watson⁴, Alun Hubbard^{1,6}, Neil F.
Glasser¹**

¹Centre for Glaciology, Department of Geography and Earth Sciences, Aberystwyth University, Aberystwyth, UK. ²Department of Biological and Environmental Sciences, University of Hertfordshire, Hatfield, UK. ³Department of Geography, University of Sheffield, Sheffield, UK. ⁴School of Geography, University of Leeds, Leeds, UK. ⁵Department of the Natural and Built Environment, Sheffield Hallam University, Sheffield, UK. ⁶Centre for Arctic Gas Hydrate, Environment and Climate, Department of Geosciences, The Arctic University of Norway, Tromsø, Norway.

* Corresponding author: Tristram Irvine-Fynn (tdi@aber.ac.uk)

Key Points:

- The monsoon season runoff hydrograph from Khumbu Glacier displays progressive changes in diurnal timing and recession characteristics.
- We propose that observed hydrological behavior results from seasonal evolution of supraglacial ponds and connections.
- Predicted expansion of debris-covered areas and pond extents will influence downstream timing, availability and quality of meltwater in the Himalaya.

Abstract

1 Meltwater and runoff from glaciers in High Mountain Asia is a vital freshwater resource for one
2 fifth of the Earth's population. Between 13% and 36% of the region's glacierized areas exhibit
3 surface debris cover and associated supraglacial ponds whose hydrological buffering roles
4 remain unconstrained. We present a high-resolution meltwater hydrograph from the extensively
5 debris-covered Khumbu Glacier, Nepal, spanning a seven-month period in 2014. Supraglacial
6 ponds and accompanying debris cover modulate proglacial discharge by acting as transient and
7 evolving reservoirs. Diurnally, the supraglacial pond system may store >23% of observed mean
8 daily discharge, with mean recession constants ranging from 31 to 108 hours. Given projections
9 of increased debris-cover and supraglacial pond extent across High Mountain Asia, we conclude
10 that runoff regimes may become progressively buffered by the presence of supraglacial
11 reservoirs. Incorporation of these processes is critical to improve predictions of the region's
12 freshwater resource availability and cascading environmental effects downstream.

13

14 **1 Introduction**

15 An estimated 1.4 billion people depend on freshwater sourced from snow and ice melt in High
16 Mountain Asia [Immerzeel *et al.*, 2010]. Although highly variable across the region, this
17 meltwater typically contributes between 20% and 50% of the total annual runoff [Bookhagen and
18 Burbank, 2010; Immerzeel and Bierkens, 2012; Lutz *et al.*, 2014]. Contemporary observations
19 [Bolch *et al.*, 2012; Kaab *et al.*, 2012; Pritchard, 2017; Brun *et al.*, 2017] and predicted trends
20 [e.g. Shea *et al.*, 2015a; Soncini *et al.*, 2016] of glaciers in the Himalaya demonstrate declining
21 ice volumes, but highlight uncertainty over the associated glacio-hydrological impacts and
22 consequent water stress arising from climate change. One important cause of this ambiguity is
23 the presence of a supraglacial debris mantle present on many of the region's glaciers, which
24 covers up to 36% of the glacierized area in the Everest region [Bolch *et al.*, 2012; Kaab *et al.*,
25 2012; Scherler *et al.*, 2011; Thakuri *et al.*, 2014]. This debris mantle commonly causes
26 downglacier ablation areas to exhibit low surface gradients and velocities [e.g. Quincey *et al.*
27 2007; Scherler *et al.*, 2011; Thompson *et al.*, 2016; Salerno *et al.*, 2017] and its overall extent is
28 increasing and predicted to expand further [Rowan *et al.*, 2015; Thakuri *et al.*, 2014; Bolch *et al.*,
29 2008]. Supraglacial debris exerts a critical influence on glacier response to climate forcing
30 because, dependent on its thickness, debris can either accelerate or retard ablation [Østrem 1959;
31 Evatt *et al.*, 2015]. This effect, coupled with the dynamic topography of the glacier surface,
32 promotes highly heterogenous ablation and the formation of surface lakes and ponds, which are a
33 common feature of receding debris-covered glaciers [Reynolds, 2000; Benn *et al.*, 2012;
34 Gardelle *et al.*, 2011; Watson *et al.*, 2016; Bassnet *et al.*, 2013; Miles *et al.*, 2016, 2017a,b;
35 Narama *et al.*, 2017]. However, the processes and causal relationships underpinning the spatial
36 distribution of supraglacial ponds remain unclear [Salerno *et al.*, 2017].

37 Supraglacial ponds are 'hotspots' of glacier ablation [Mertes *et al.*, 2016] due to their reflective
38 and thermal characteristics [Sakai *et al.*, 2000; Benn *et al.*, 2001; Miles *et al.*, 2016; Watson *et*
39 *al.*, 2017a] and the presence of bare-ice cliffs associated with pond formation and growth [Sakai
40 *et al.*, 2002; Brun *et al.*, 2016; Watson *et al.*, 2017b]. Consequently, ponds may accelerate glacier
41 thinning and recession and act as temporary meltwater storage reservoirs [Benn *et al.*, 2001,
42 2012]. Ponds on debris-covered glaciers are commonly either transient features due to inception
43 or collapse of near-surface or shallow englacial drainage routes and consequent drainage, or

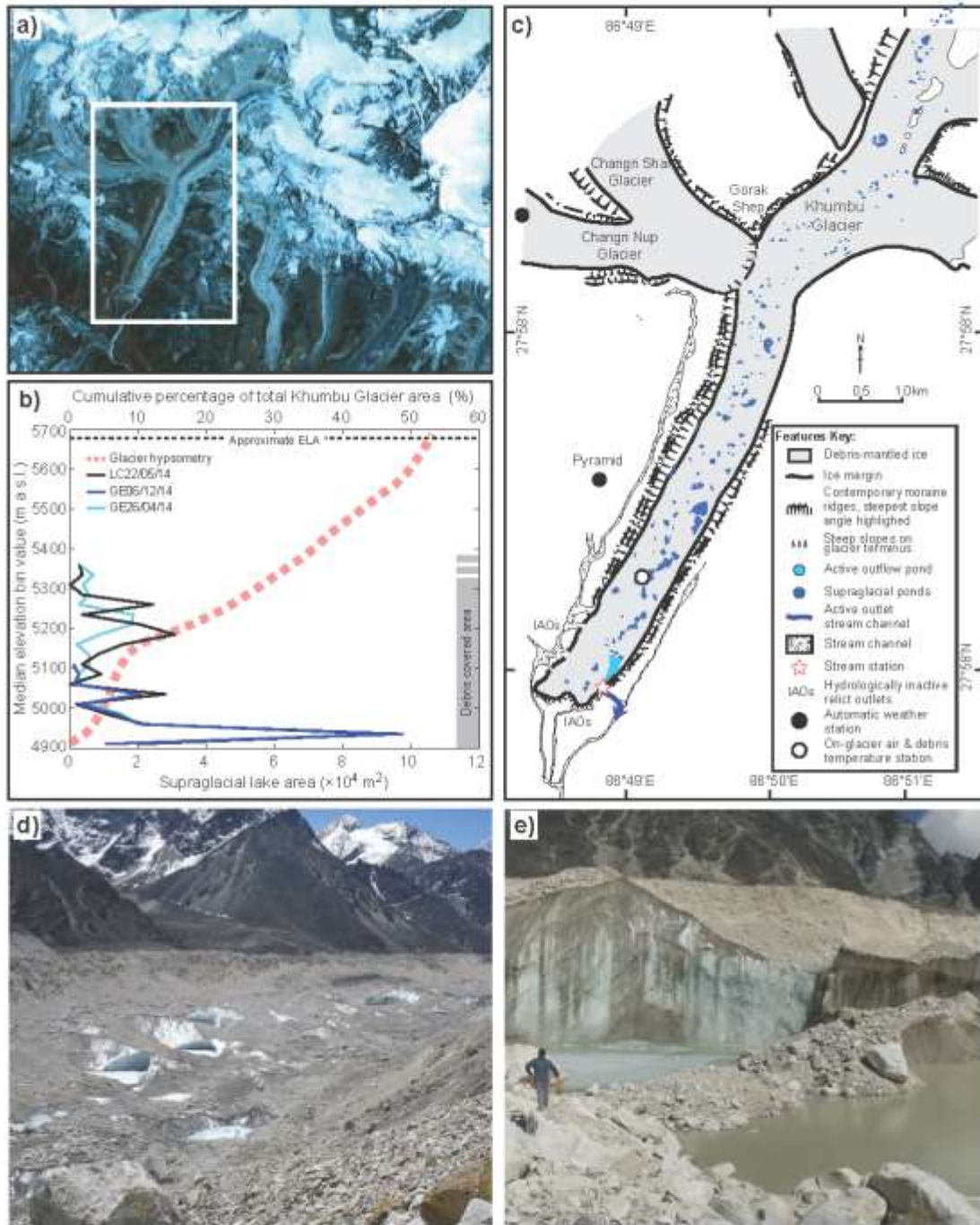
44 appear ‘perched’ in closed basins where efficient flowpaths are absent [*Reynolds, 2000; Benn et*
45 *al., 2001; Miles et al., 2017b; Watson et al., 2017a*]. Seasonally, ponds on Himalayan glaciers
46 typically grow both in area and depth [*Watson et al., 2017a*], attaining maximum extent mid-
47 monsoon and declining in size thereafter [*Miles et al., 2017a; Narama et al., 2017; Watson et al.,*
48 *2016*]. Inter-annually, debris redistribution and change in surface topography results in variation
49 in pond positions [*Narama et al., 2017; Watson et al., 2016*] and as ponds attain their local
50 hydrological base-level they may evolve into larger scale lakes [*Thompson et al., 2016; Mertes et*
51 *al., 2016*]. Observations of supraglacial pond water quality confirm that hydrological linkages do
52 exist between ponds [*Takeuchi et al., 2000; Bhatt et al., 2016*], and pond extent may be governed
53 by the evolving development and (re)organization of supraglacial drainage systems [*Watson et*
54 *al., 2016, 2017a; Miles et al., 2017b*]. Yet the extent to which these ponds impact upon
55 meltwater generation and modify the seasonal hydrograph remains poorly quantified.

56 A lack of *in situ* observations of meltwater generation, transit and runoff for Himalayan glaciers
57 [*Immerzeel et al., 2012; Bajracharya et al., 2015*] has led to uncertainties in the prediction of
58 their hydrological response to environmental forcing. For example, some numerical models of
59 debris-covered glacier systems utilize a linear reservoir parameterization linking proglacial
60 discharge to meltwater production [e.g. *Ragettli et al., 2015; Fujita and Sakai, 2014*]. Such
61 methods though fail to account for the potential hydrological complexities in the region.
62 Specifically, the presence of interconnected supraglacial ponds implies a potentially complex
63 hydrological system [*Miles et al., 2017b*] that will modulate the water inputs to, and outputs from
64 the glacier system. Hence, the acquisition of detailed measurements characterizing the
65 hydrological behavior of debris-covered glaciers on diurnal to seasonal timescales is an
66 imperative for improved predictions of meltwater delivery to downstream water resources
67 throughout the Himalaya. Here, we present the results of a glacier-scale runoff monitoring
68 program at the debris-covered Khumbu Glacier in the Everest region of Nepal. Our
69 measurements span a 190-day period from April to November 2014 including the summer
70 monsoon season.

71 **2 Field Site and Methods**

72 Khumbu Glacier (27.97°N, 86.83°E) flows from the southern flanks of Mount Everest to its
73 terminus at ~4900 m a.s.l. (Figure 1a). The terminus elevation is slightly lower than the local

74 permafrost limit of ~5000 m a.s.l. [Schmid *et al.*, 2015]. The glacier is likely to be polythermal,
75 with an estimated 17 m deep cold surface ice layer [Mae *et al.*, 1975]. The glacier thinned at
76 approximately -0.6 m a^{-1} between 2000 and 2015, with losses of -1.4 m a^{-1} at elevations of
77 5200–5300 m [King *et al.*, 2017]. Approximately 47% of the 41 km² glacier including the
78 Changri Nup and Changri Shar tributaries is debris-covered (Figure 1b). Supraglacial debris
79 thickness varies from 0.1 m to over 3 m and is concentrated over the lowermost 8 km of the
80 glacier [Soncini *et al.*, 2016], overlying 20 m to 440 m of glacier ice [Gades *et al.*, 2000]. Recent
81 observations [e.g. Nuimura *et al.*, 2011] indicate that this debris cover has become increasingly
82 topographically uneven: differential ablation has resulted in a complex glacier surface
83 characterized by the presence of numerous supraglacial water bodies [Wessels *et al.*, 2002;
84 Watson *et al.*, 2016]. Throughout 2014, ~1% of the total debris-covered area comprised
85 supraglacial ponds (Figures 1b-e). However, as elsewhere in the region, the hydrological
86 evolution and connectivity of these supraglacial ponds is poorly constrained. The Changri Nup
87 and Changri Shar tributaries are now physically disconnected, but retain a surface hydrological
88 connection with the Khumbu Glacier tongue [Vincent *et al.*, 2016]. The only visible source of
89 meltwater runoff flowing from the Khumbu catchment emerges from a turbid supraglacial lake
90 situated close to the eastern glacier margin (Figure 1c). There is no evidence of alternative,
91 active terminal or lateral outlets for englacial or subglacial drainage pathways. Runoff data were
92 recorded immediately downstream of this outlet lake, where meltwater drains via a breach in the
93 eastern Little Ice Age lateral moraine to the upper Dudh Koshi.



94 **Figure 1:** (a) ASTER imagery (Sept 2012) of the Everest region, Nepal, outlining lower
95 elevations of the Khumbu Glacier detailed in (c); (b) hypsometry and supraglacial pond area in
96 Khumbu Glacier ablation zone based on satellite imagery from 26 April, 22 May and 6
97 December 2014 [see *Watson et al.*, 2016]; (c) ablation zone of Khumbu Glacier highlighting key
98 data collection sites and major geomorphological features, including hydrologically inactive
99 outlets (IAOs) indicative of abandoned drainage routes and supraglacial lake positions on 26
100 April 2014 prior to the onset of the monsoon season; (d, e) oblique images illustrating typical
101 debris cover and pond morphology, taken during the pre-monsoon period, May 2014.

102

103 Discharge (Q) data were collected between 14 May and 12 November (Day of Year (DOY) 135
104 to 317) using standard methods [*Herchy*, 1995]. A hydrological monitoring station was
105 established in a stable reach of the sole outflow channel at 4930 m a.s.l.. Average water stage
106 was recorded at 30 min intervals using a Druck PDCR1730 pressure transducer and Campbell
107 Scientific (CS) CR1000 data logger. A stage-discharge rating curve was developed using
108 triplicate dilutions [*Hudson and Fraser*, 2005] of 3 mL aliquots of 10% fluorescein and a Turner
109 Designs Cyclops7 fluorometer linked to a CS CR10X datalogger. A non-linear stage-discharge
110 relationship yielded a coefficient of determination of $r^2 = 0.79$ ($n = 18$). Estimated uncertainty in
111 Q is <15%, although this is increased for higher Q values [see *Supplementary Information*; *Rantz*
112 *et al.*, 1982; *Sakai et al.*, 1997; *DiBaldassarre and Montanari*, 2009]. On-glacier air temperature
113 (T_a) and debris temperature (T_d) were monitored at 4935 m a.s.l. using Gemini TinyTag2 logging
114 thermistors with a stated measurement accuracy of $\pm 0.4^\circ\text{C}$ (Figure 1c). The T_a sensor was
115 mounted in a naturally aspirated radiation shield 1 m above the debris surface; the T_d sensors
116 were located within the debris layer at depths of 0.55 and 1.0 m below the surface and away from
117 the debris-ice interface. All temperature measurements were recorded at 30-min intervals. Local
118 incident shortwave radiation (SW_{in}) was recorded at an automatic weather station 5363 m a.s.l.
119 on the Changri Nup Glacier (Figure 1c) using a Kipp & Zonen CNR4 sensor with 3%
120 uncertainty. Precipitation (P) was measured at Pyramid Observatory (Figure 1c) at 5035 m a.s.l.
121 using a Geonor T-200 gauge; these hourly data were corrected for undercatch of solid
122 precipitation and have an estimated accuracy of $\pm 15\%$ [*Sherpa et al.*, 2017].

123 We examined the timing of peak discharge and the shape of the diurnal hydrograph using
 124 standard approaches; lag times between time-series were identified using a moving window
 125 cross-correlation [e.g. *Jobard and Dzikowski, 2006*], while we classified diurnal hydrographs
 126 using a paired Principal Components Analysis (PCA) and Hierarchical Cluster Analysis (HCA)
 127 approach [e.g. *Hannah et al., 2000; Swift et al., 2005*]. Specifically, daily (24 hr) hydrographs
 128 were assumed to commence at low Q at 06:00, PCA was conducted without rotation and only
 129 components with eigenvalues > 1.0 were retained. PCA identified modes of diurnal Q variation
 130 defined by the standardized component loadings and these loadings for each day were clustered
 131 using Euclidean distance measures and a within-groups linkage method. A total of 6 groups were
 132 identified and further classified using a second, independent HCA that defined diurnal
 133 hydrograph similarity based on key discharge metrics following z-score normalization. Daily
 134 hydrographs were then described based on ‘shape’ defined by PCA clusters and ‘magnitude’
 135 identified in the secondary HCA.

136 Estimates of recession storage constants (K) for each diurnal hydrograph were derived from
 137 semi-logarithmic plots of Q versus time [e.g. *Gurnell, 1993; Hodgkins et al., 2013*] where:

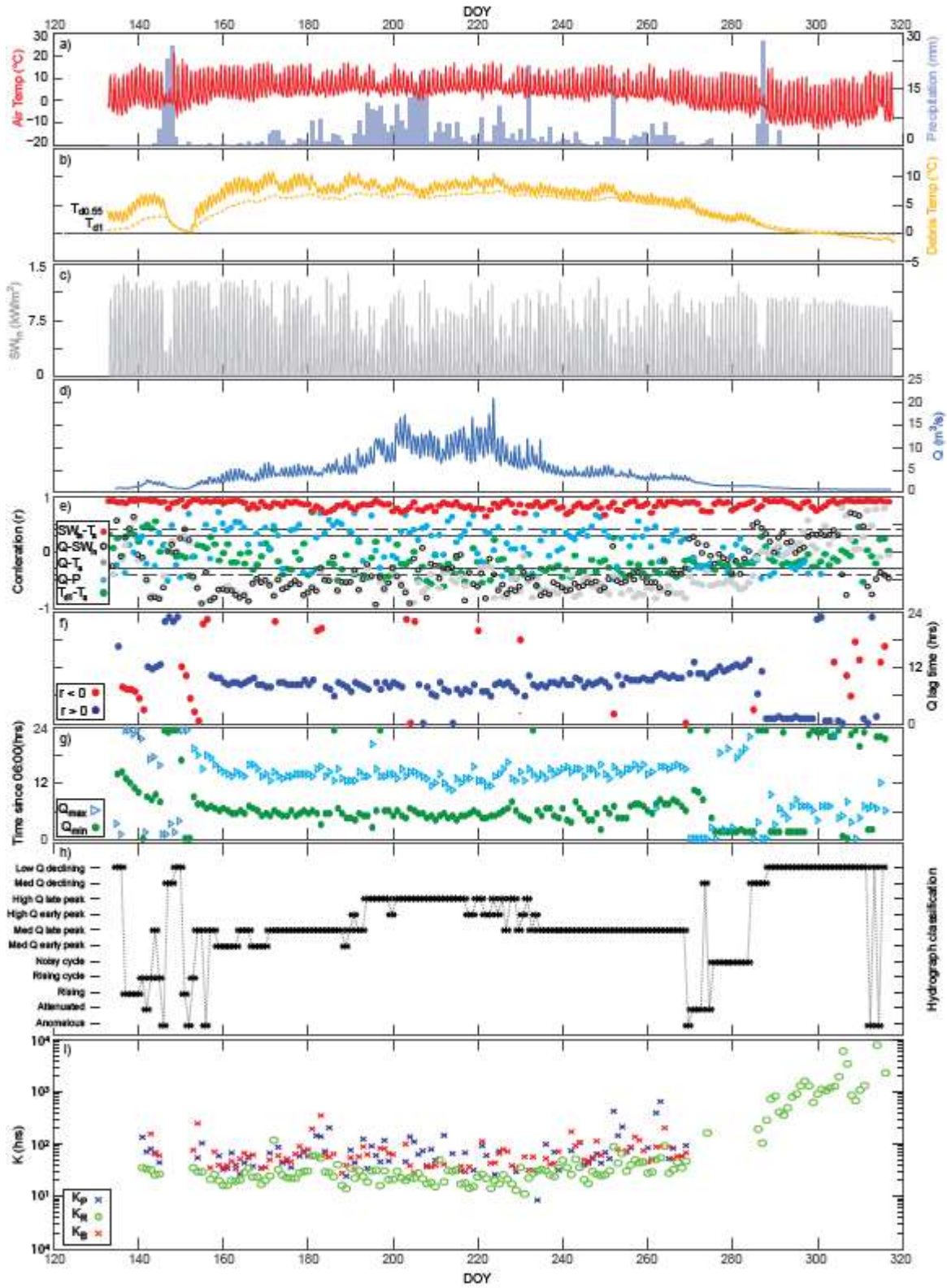
$$138 \quad \mathbf{K} = \frac{-t}{\ln\left(\frac{Q_t}{Q_0}\right)} \quad \text{Eq.1}$$

139 for which t is time since the start of the recession segment, and Q_0 and Q_t the discharge at the
 140 start of the recession segment and at time t , respectively. For all days classified as exhibiting
 141 diurnal discharge cycles ($n = 117$) or constant recessional hydrographs ($n = 29$), K-values were
 142 calculated from the time-step following peak discharge, or from 18:00 in the case of persistent
 143 recession hydrographs. Recession segments and associated aggregate recession constants were
 144 identified using segmented linear regression for cases exhibiting durations >1 hr.

145 **3 Results**

146 The meteorological and discharge time-series (Figure 2a-d) for the 2014 monsoon season reveal
 147 that T_a and SW_{in} exhibited strong diurnal variations, with highest incident energy fluxes between
 148 10:00 and 15:00, as typifies the region [see *Shea et al., 2015b*]. These two variables were highly
 149 correlated over the diurnal cycle ($r > 0.5$, $p < 0.05$) throughout the observation period (Figure

150 2e). Seasonal changes in T_d aligned well with T_a , although at the daily timestep, correlation
151 suggested a changing lag between variables (Figure 2e). Despite a distinct diurnal variability in
152 T_d , variation was suppressed at depth (Figure 2b), and T_d remained below 0°C following DOY
153 300. The seasonal pattern of Q broadly followed that of T_a with an underlying diurnal fluctuation
154 of between 0.005 and $12.3 \text{ m}^3 \text{ s}^{-1}$, and daily mean Q peaking at $\sim 9 \text{ m}^3 \text{ s}^{-1}$ which compares well
155 with published records of discharge during 2014 for the upper Dudh Koshi [*Soncini et al.*, 2016;
156 see *Supplementary Information*]. Interestingly, diurnal correlation indicated Q and both T_a and
157 SW_{in} vary out of phase for much of the observation period (Figure 2e). Q lagged T_a progressively
158 decreasing from 12 to 6 hrs until DOY 220, and subsequently returning to lags >12 hrs until
159 DOY 285 when lags dropped again to ~ 6 hrs (Figure 2f). The diurnal hydrograph cycle became
160 steadily delayed until DOY270 when T_d declined to $\sim 5^\circ\text{C}$ and continued to fall when a
161 protracted hydrograph recession dominated. While statistically significant diurnal correlations
162 between Q and P were found, these were inconsistent and showed no systematic trend (Figure
163 2e). Lag analysis highlighted statistically significant correlations ($r > 0.405$, $p < 0.05$) between Q
164 and P over 24 hr periods, predominantly with Q lagged by >10 hrs, however no pattern in lag
165 time was observed.



167 **Figure 2:** Time-series of (a) on-glacier air temperature T_a and total daily precipitation P , (b)
168 debris temperature T_d at 0.55 and 1.0 m below the debris surface, (c) incident shortwave
169 radiation SW_{in} and (d) meltwater discharge Q . Analyses identify (e) daily correlations between
170 T_a , SW_{in} , P and Q with the 95% confidence levels indicated for the hourly ($r \approx 0.41$) and half-
171 hourly ($r \approx 0.29$) data sets, (f) the lag time between daily peak T_a and maximum Q , (g) the timing
172 of minimum and maximum Q , (h) the daily hydrograph classification based on shape and
173 magnitude, and (i) the three principal hydrograph recession constants (K_P , K_R and K_B).

174

175

176 Three sequential recession segments were identified as typical within the time-series: (i) slow
177 decrease in Q lasting ≤ 7 hours immediately following peak Q (K_P), (ii) major recession
178 component of rapid decrease in Q over ~ 9 hours duration (K_R), and (iii) a second slow decrease
179 for ~ 5 hours prior to the onset of the next diurnal cycle (K_B). Where only a singular extended
180 recession was identified, this was taken to be K_R . K_P and K_B were found to be statistically
181 similar, but lacked a significant temporal trend, while K_R showed a strong non-linear association
182 with peak Q , decreasing and increasing as the monsoon season progressed. While aggregate K -
183 values broadly agree with the magnitude of those identified in other glacial runoff records (mean
184 $K_P = 86.7$ and $K_B = 72.4$ hrs, while mean $K_R = 108$ hrs for the season, but 31.1 hrs before
185 DOY270), the recession segment pattern contrasts with the commonly reported systematic
186 increase in K -values over diurnal hydrograph recession segments [e.g. *Gurnell, 1993; Hodgkins*
187 *et al., 2013*]. No association between K -values and P or daily peak Q was found. In tests,
188 uncertainty related to the rating curve used to derive the Q time-series [see *Supplementary*
189 *Information; Rantz et al., 1982*] did not impact the recession patterns identified; however, if
190 using a power-law rating curve [*Herchy, 1995*], recession constants K_P , K_R and K_B increased by
191 $81 \pm 30\%$, $51 \pm 50\%$ and $57 \pm 26\%$ respectively.

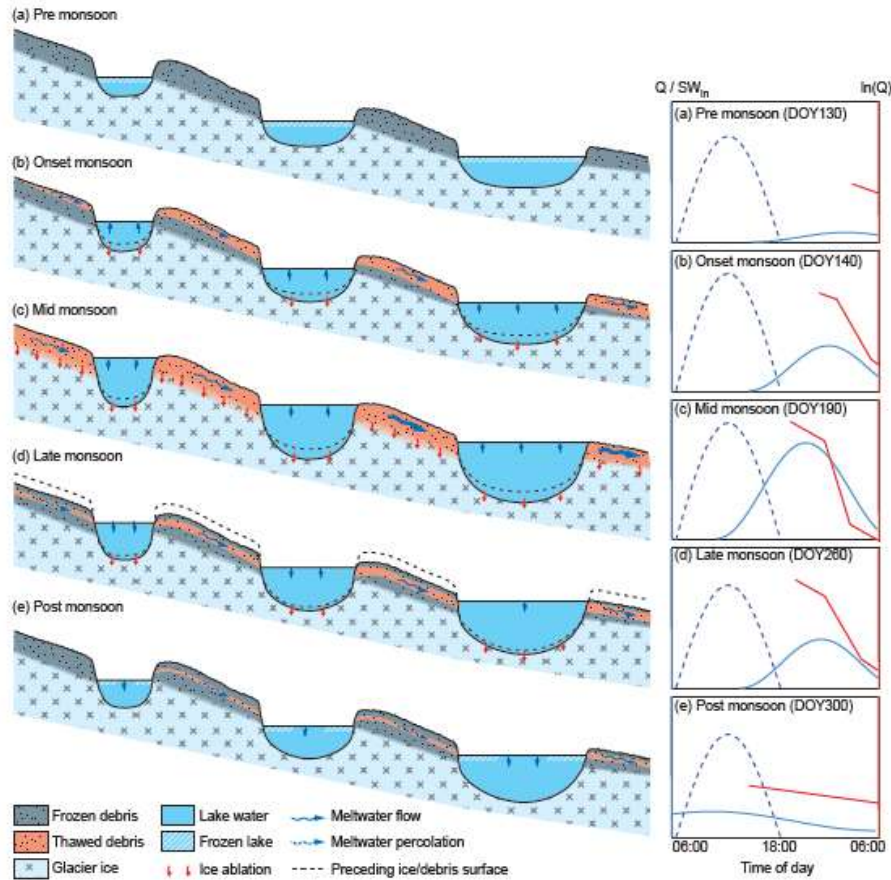
192 **4 Discussion**

193 Our results from Khumbu Glacier indicate a hydrological configuration with both similarities
194 and distinct differences to those typically reported for Alpine glacier systems in Europe and

195 elsewhere. Systematic progression in timing of peak Q, seasonal undulation in diurnal discharge
196 amplitude, diurnal hydrograph asymmetry, and clear patterns in hydrograph classification are
197 commonly described for temperate, debris-free alpine glaciers [e.g. *Richards et al.*, 1996;
198 *Hannah et al.*, 2000; *Swift et al.*, 2005; *Jobard and Dzikowski*, 2006]. Typically, as the snowline
199 recedes upglacier and melt season advances, peak Q occurs progressively closer to the time of
200 heightened SW_{in} and T_a and, even for large south-facing valley glaciers such as Aletschgletscher,
201 equivalent in size to Khumbu Glacier, Q lags the meteorological drivers of melt by <5 hrs during
202 much of the ablation season [e.g. *Lang*, 1973; *Verbunt et al.*, 2003]. As ablation continues on
203 debris-free glaciers, the amplitude of Q increases, and the hydrograph form becomes more
204 accentuated. Here, particularly prior to DOY230 (Figures 3f-h), the patterns of hydrograph
205 characteristics resemble those reported for temperate alpine settings.

206 However, in contrast to debris-free alpine counterparts, the timing of daily peak and minimum
207 discharge at Khumbu Glacier shows a more marked delay relative to meteorological drivers of
208 ablation: peak Q occurs ≥ 6 hours after maximum SW_{in} and T_a , while minimum Q commonly
209 coincides with peak irradiance. Q lagging energy fluxes reflects the delay in energy transfers that
210 initiate melt, particularly for those associated with exchange at the atmosphere-debris interface
211 and through the debris layer [*Carenzo et al.*, 2016] (Figure 2b). Further lags may relate to
212 meltwater transit to the monitoring site. Transition in lag time between T_a and Q mid-season is
213 ascribed to changes in weather systems and lapse rates reported for the region during the
214 monsoon [e.g. *Shea et al.*, 2015b, *Steiner and Pellicciotti* 2016], the reduction in both T_a and
215 SW_{in} , and subtle changes in the hydrological function of the drainage system. The lack of
216 association between Q and precipitation has been observed elsewhere on debris-covered glaciers
217 [e.g. *Thayyen et al.*, 2005]. However, the elongated diurnal hydrograph recession diverges
218 notably from other glacial observations and more specifically recession data reported here
219 evidence neither ‘fast’ supraglacial and ‘moderate’ en- and sub-glacial drainage flowpaths,
220 superimposed on a ‘slow’ persistent baseflow on a diurnal basis, nor a seasonal decline in
221 recession storage constants [cf. *Gurnell*, 1993]. Furthermore, the gauging station elevation (4930
222 m a.s.l.), ensures the Q record solely relates to the supraglacial (debris-covered) and shallow
223 englacial environment. Observations during 2014 confirmed that some supraglacial meltwaters
224 entered a shallow englacial network, potentially allowing flow between supraglacial ponds,
225 evidenced by spatial variability in pond turbidity which suggested hydrological connectivity

226 (Figure 1e) [see *Takeuchi et al.*, 2012]. While geomorphic signatures suggested that meltwater
227 that had once drained or followed seepage pathways through other moraine breach locations,
228 contemporary field observations indicate these are relict inactive features (IAOs: Fig. 1c).
229 Consequently, we discuss our data in the context of a conceptual model of the dominantly
230 supraglacial drainage system illustrated in Figure 3, comprising a debris layer punctuated by a
231 cascade of lakes or ponds.



232 **Figure 3:** Conceptual model of the seasonal hydrological development of the surface of a
 233 Himalayan debris-covered glacier over an annual cycle. Indicative daily hydrometeorological
 234 plots for each stage are shown with SW_{in} (dashed), Q (blue), and a natural logarithmic
 235 transformed Q used to identify the recession components (red). Pre-monsoon (a) the surface is
 236 frozen following the winter period, but as the monsoon season approaches (b), the debris-cover
 237 begins to thaw, and water derived from melting intra-clast ice and ponds commences flow and
 238 thermal ablation at the base of ponds. Mid monsoon (c) the debris is fully thawed, ponds become
 239 connected and glacier ice melt occurs and ponds deepen through thermal ablation, which,
 240 coupled with monsoon rainfall, leads to more efficient drainage over the glacier ice surface.
 241 Towards the end of the monsoon season (d) the air temperatures drop and initiate freezing at the
 242 debris surface, while reductions in water flow facilitate upward freezing at the base of the debris
 243 layer; however, the thawed portion of the debris layer still transfers meltwater from ponds
 244 towards the glacier margin, albeit delayed. Post monsoon (e), which aligns with the latter portion

245 of our records, continued freeze-up of the lake and debris layer occurs restricting any
246 transmission of meltwater as winter approaches and the glacier-wide hydrological system drains.

247

248 The cascade of developing ponds represents a series of reservoirs capable of temporarily storing
249 meltwater and delaying its transit downstream. Combining the pre-monsoon pond areas (\sim
250 $2.5 \times 10^5 \text{ m}^2$; Figure 1) with observation of the outflow lake level varying by $\sim 0.7 \text{ m}$ over a
251 diurnal melt cycle, we estimate the supraglacial pond cascade on Khumbu Glacier to account for
252 a minimum daily storage capacity of $\sim 1.75 \times 10^5 \text{ m}^3$ (equivalent to 23% of the observed mean
253 daily discharge). Supported by evidence of progressive pond deepening during the monsoon
254 season [e.g. *Watson et al.*, 2017a] we conclude that the diurnal storage capacity of the pond
255 system alone, not including the porous debris layer, can readily accommodate the observed daily
256 mean P ($\sim 1.23 \times 10^5 \text{ m}^3$ over the whole glacier area). The timing and magnitude of on-glacier
257 storage may also be controlled by freeze-thaw processes, analogous to a periglacial environment
258 given the local permafrost limit. During the winter, both the supraglacial debris layer and ponds
259 are largely frozen, likely becoming impermeable and unable to convey any surface meltwater. As
260 the monsoon season develops, the system progressively thaws [e.g. *Sakai et al.*, 2000; *Benn et*
261 *al.*, 2001; *Namara et al.*, 2017; *Miles et al.*, 2016; *Watson et al.*, 2017a]. The ponds may become
262 hydrologically linked by three key flowpaths: those within the debris-covered mantle; shallow
263 debris-filled crevasses [e.g. *Benn et al.*, 2012; *Gulley and Benn*, 2007] or channels formed from
264 collapsed near-surface englacial conduits [*Miles et al.*, 2017b]; or debris- or water-choked near-
265 surface passages [*Watson et al.*, 2017a]. Published figures for heterogeneous debris indicate
266 permeability of between 10^{-2} to 10^{-6} m s^{-1} [*Parriaux and Nicoud*, 1990; *Muir et al.*, 2011; *Woo*
267 *and Steer*, 1983; *Gulley and Benn*, 2007] although mobilization of fines may further reduce
268 hydraulic efficiency [*Woo and Xia*, 1995]. When thawed, therefore, we anticipate the debris
269 layer and associated supraglacial and shallow or collapsed englacial features may act as a depth-
270 limited, transient storage reservoir, regulating bulk meltwater discharge over the glacier surface
271 and between ponds and hence moderating the overall diurnal flow variance. The debris layer is
272 underlain by glacier ice with discrete, spatially limited, shallow englacial flowpaths analogous to
273 continuous permafrost with isolated, closed talik. The result, in the monsoon-influenced climate,
274 is a thermal regime dominated by the seasonal freezing and thawing of the debris layer, as is

275 evident in our T_d time-series, and for which the correlations between T_a and T_d (Figure 2e) likely
276 reflect change in debris heat capacity with water content. Khumbu Glacier's supraglacial debris
277 layer may therefore be considered equivalent to a seasonally cryotic active layer [Bonnaventure
278 and Lamoureux, 2013].

279 As the monsoon season progresses, evolution of the debris mantle hydrological system may
280 result in increased inter-pond connectivity. Progressive thaw at depth in the debris layer and
281 glacier ice melt, despite enlarging the supraglacial storage capacity, also aids the development of
282 increasingly efficient supra-permafrost drainage: inter-clast ice is replaced with water flow
283 pathways and increased hydraulic permeability [Woo and Steer, 1983; Woo and Xia, 1995],
284 providing more efficient connections through the debris and facilitating debris-ice interface and
285 englacial flowpath development [Gulley and Benn, 2007; Gulley et al., 2009; Miles et al., 2017b;
286 Watson et al., 2017a]. Strengthening connectivity increases the rapidity of runoff through the
287 cascading pond system. Sporadic activation, modification or abandonment of flowpaths and
288 diurnal or seasonal variation in supraglacial pond storage capacity likely contributes to the
289 observed variation of discharge recession (Fig. 3i). Such delay, peak flow suppression and
290 attenuated recession, as seen in our data, are indicative of level-pool routing controlling
291 meltwater transfer through a series of reservoirs [Montaldo et al., 2004] and, as such, the ponds
292 may be conceptualized as thermokarst [Kirkbride, 1993].

293 Evidence for this role of supraglacial ponds and debris as regulators of meltwater discharge is
294 exemplified by the diurnal hydrograph recession. When pond levels are at their peak or minima
295 at seasonal and diurnal time-scales, K_P and K_B are determined by the hydraulic conductivity of
296 the (thawed) debris that separates the individual pond basins. K_P was not clearly associated with
297 either T_a or SW_{in} nor with daily maximum discharge; the recession segment was not associated
298 with the magnitude of meltwater production. Once daily meltwater provision declines or ceases,
299 changes in hydraulic head drive drainage through the pond cascade and the major recession (K_R)
300 is governed by outflow channel geometry rather than rates of inflow controlled by debris
301 permeability. K_R remains broadly consistent over the hydrologically active period (DOY134-
302 270). Subsequently, particularly as T_a and T_d both fall and water drains from the pond cascade,
303 water within the debris layer and debris-rich hydraulic connections between ponds refreezes, and

304 the hydraulic efficiency of the system declines. This change is highlighted by $K_R > K_B$, the post-
305 monsoon increase in K_R and a strongly negative, non-linear relationship between K_R and peak Q .

306 The observations following DOY 230 of declining Q despite positive T_a and T_d and precipitation
307 contributions are counterintuitive. However, given our hydrological analysis and conceptual
308 model it seems reasonable to suggest that this effect could have arisen from the fully thawed
309 debris layer readily storing excess water produced in this period and mobilization of fines
310 impinging on hydrological efficacy, with a consequent net reduction in throughflow evidenced
311 by gradual increases in all K -values. The drainage of meltwater continued for ~45 days after
312 night time T_a dropped to freezing, with around 7% of the observed runoff volume being
313 delivered in this late- and post-monsoon period. This protracted drainage corresponds well to the
314 delay in runoff thought to relate to hysteresis caused by a deep groundwater system in the Nepal
315 Himalaya [Andermann *et al.*, 2012]. Our data suggest that widespread supraglacial debris layers
316 themselves may contribute to the observations of reservoir behavior in glacierized catchments at
317 a seasonal timescale, and extend the duration of glacier meltwater delivery to downstream
318 environments.

319 **5 Conclusions**

320 We have demonstrated that the evolving system of supraglacial ponds and accompanying debris
321 has the capacity to act as a fundamental modulator of proglacial discharge regimes at Khumbu
322 Glacier. Although there is uncertainty in the causal associations between glacier surface gradient,
323 debris cover and pond occurrence [Salerno *et al.*, 2017], supraglacial ponds are reported to be
324 increasingly prevalent on debris-covered glaciers and represent an active and dynamic
325 hydrological system [Miles *et al.*, 2017a,b; Narama *et al.*, 2017; Watson *et al.*, 2016, 2017a].
326 Recently, there has been growing recognition that small changes in hydrological function in
327 mountain regions can have substantial impacts on freshwater availability [e.g. Pritchard, 2017]
328 and biodiversity [Jacobsen *et al.*, 2012] in terrestrial water bodies and ecosystems in the
329 Himalaya [Xu *et al.*, 2009; Salerno *et al.*, 2016]. To understand the hydrological response of
330 debris-covered glaciers and to forecast changes in water resources and ecosystem services in the
331 region, it is crucial to explicitly incorporate processes relating to the thermodynamics and
332 hydrology of widespread debris mantles that can now be considered as cryotic, thermokarstic
333 active layers – systems that are more commonly described solely in periglacial settings

334 [Bonnaventure and Lamoureux, 2013]. Further geophysical and hydrochemical exploration of
335 debris cover [e.g. Muir *et al.*, 2011; McCarthy *et al.*, 2017] is needed to better define the nature
336 of the supraglacial debris-covered drainage system and the modes and thermodynamics of
337 hydraulic connectivity between ponds. With ~75 to 90% glacier area in the Himalaya above
338 4500–5000 m a.s.l., the elevation range commonly associated with the regional permafrost limit
339 [Schmidt *et al.*, 2015], processes we describe here should be widely applicable throughout the
340 region and highlight the important role that debris-layer supraglacial hydrology may have on
341 mediating glacier runoff characteristics in High Mountain Asia. Long-term increases in areal
342 extent of debris cover and ponds will not only contribute to more rapid glacier mass loss but, we
343 propose, also alter patterns of meltwater supply and quality to downstream catchments through
344 their roles as temporary reservoirs and flow regulators. A more complete understanding of this
345 buffering process is crucial to improving projections of the region's future water resources in a
346 changing climate.

347

348 **Acknowledgments and Data**

349 All authors acknowledge the Royal Society (Research Grant: RG120393) and the British Society
350 for Geomorphology. Summit Treks provided logistical support in Nepal. Patrick Wagon kindly
351 provided incident radiation and precipitation data. TDI, PRP, NFG and JWB led the analysis,
352 writing and conceptual development. TDI, AVR, DJQ and MJG undertook fieldwork in Nepal.
353 PRP provided fieldwork equipment and instruments. CSW acquired and processed supraglacial
354 lake data. All authors contributed to development, editing and revision of the final manuscript.
355 We thank the two reviewers who both provided insightful suggestions to help improve the paper.

356 All new data presented here are available via www.pangaea.de :

357 doi.org/10.1594/PANGAEA.883071 and doi.org/**XXXXXXXX**

358

359 **References**

360 Andermann, C., L. Longuevergne, S. Bonnet, A. Crave, P. Davy and R. Gloaguen (2012). Impact
361 of transient groundwater storage on the discharge of Himalayan rivers. *Nature*
362 *Geoscience*, 5, 127-132.

- 363 Bajracharya, S.R, S.B. Maharjan, F. Shrestha, W. Guo, S. Liu, W. Immerzeel and B. Shrestha
364 (2015). The glaciers of the Hindu Kush Himalayas: current status and observed changes
365 from the 1980s to 2010. *International Journal of Water Resources Development*, 31, 161-
366 173.
- 367 Basnett, S., A.V. Kulkarni, and T. Bolch (2013). The influence of debris cover and glacial lakes
368 on the recession of glaciers in Sikkim Himalaya, India. *Journal of Glaciology*, 59, 1035-
369 1046.
- 370 Benn, D.I., T. Bolch, K. Hands, J. Gulley, A. Luckman, L.I. Nicholson, D. Quincey, S.
371 Thompson, R. Toumi and S. Wiseman (2012). Response of debris-covered glaciers in
372 the Mount Everest region to recent warming, and implications for outburst flood hazards.
373 *Earth-Science Reviews*, 114, 156-174.
- 374 Benn, D.I., S. Wiseman, and K.A. Hands (2001). Growth and drainage of supraglacial lakes on
375 debris mantled Ngozumpa Glacier, Khumbu Himal, Nepal. *Journal of Glaciology*, 47,
376 626-638.
- 377 Bhatt, M.P., N. Takeuchi and M.F. Acevedo (2016). Chemistry of Supraglacial Ponds in the
378 Debris-Covered Area of Lirung Glacier in Central Nepal Himalayas. *Aquatic*
379 *Geochemistry*, 22(1), pp.35-64.
- 380 Bolch, T., M. Buchroithner, T. Pieczonka and A. Kunert (2008). Planimetric and volumetric
381 glacier changes in the Khumbu Himal, Nepal, since 1962 using Corona, Landsat TM and
382 ASTER data. *Journal of Glaciology*, 54, 592-600.
- 383 Bolch, T., A. Kulkarni, A. Kääb, C. Huggel, F. Paul, J.G. Cogley, H. Frey, J.S. Kargel, K. Fujita,
384 M. Scheel and S. Bajracharya (2012). The state and fate of Himalayan glaciers. *Science*,
385 336, 310-314.
- 386 Bonnaventure, P.P. and S.F. Lamoureux (2013). The active layer: A conceptual review of
387 monitoring, modelling techniques and changes in a warming climate. *Progress in*
388 *Physical Geography*, 37, 352-376.
- 389 Bookhagen, B. and D.W. Burbank (2010). Toward a complete Himalayan hydrological budget:
390 Spatiotemporal distribution of snowmelt and rainfall and their impact on river
391 discharge. *Journal of Geophysical Research: Earth Surface*, 115(F3), F03019.
- 392 Brun, F., E. Berthier, P. Wagnon, A. Kääb, D. Treichler, H.B. Franz, A.C. McAdam, D.W.
393 Ming, C. Freissinet, P.R. Mahaffy and D.L. Eldridge (2017). A spatially resolved
394 estimate of High Mountain Asia glacier mass balances from 2000 to 2016. *Nature*
395 *Geoscience*. doi:10.1038/ngeo2999
- 396 Brun, F., P. Buri, E.S. Miles, P. Wagnon, J. Steiner, E. Berthier, S. Ragettli, P. Kraaijenbrink,
397 W.W. Immerzeel and F. Pellicciotti (2016). Quantifying volume loss from ice cliffs on
398 debris-covered glaciers using high-resolution terrestrial and aerial photogrammetry.
399 *Journal of Glaciology*, 62, 684-695.
- 400 Carenzo, M., F. Pellicciotti, J. Mabillard, T. Reid and B.W. Brock (2016). An enhanced
401 temperature index model for debris-covered glaciers accounting for thickness effect.
402 *Advances in Water Resources*, 94, 457-469.

- 403 Di Baldassarre, G. and A. Montanari (2009). Uncertainty in river discharge observations: a
404 quantitative analysis. *Hydrology and Earth System Sciences*, 13(6), 913-921. DOI:
405 10.5194/hess-13-913-2009
- 406 Evatt, G.W., I.D. Abrahams, M. Heil, C. Mayer, J. Kingslake, S.L. Mithcel, A.C. Flower and
407 C.D. Clark (2015). Glacial melt under a porous debris layer. *Journal of Glaciology*. 61,
408 825-836.
- 409 Fujita, K. and A. Sakai (2014). Modelling runoff from a Himalayan debris-covered glacier.
410 *Hydrology and Earth System Sciences*, 18, 2679–2694.
- 411 Gades, A., H. Conway, N. Nereson, N. Naito and T. Kadota. (2000). Radio echo-sounding
412 through supraglacial debris on Lirung and Khumbu Glaciers, Nepal Himalayas. *IAHS*
413 *Publication*, 264, 13-24.
- 414 Gardelle, J., Y. Arnaud and E. Berthier (2011). Contrasted evolution of glacial lakes along the
415 Hindu Kush Himalaya mountain range between 1990 and 2009. *Global and Planetary*
416 *Change*, 75, 47-55 (2011).
- 417 Gulley, J. and D.I. Benn (2007). Structural control of englacial drainage systems in Himalayan
418 debris-covered glaciers. *Journal of Glaciology*, 53, 399-412.
- 419 Gulley, J.D., D.I. Benn, D. Müller and A. Luckman (2009). A cut-and-closure origin for
420 englacial conduits in uncrevassed regions of polythermal glaciers. *Journal of Glaciology*,
421 55, 66-80.
- 422 Gurnell A.M. (1993). How many reservoirs? An analysis of flow recessions from a glacier basin.
423 *Journal of Glaciology* 39, 132-134.
- 424 Hannah, D.M., B.P. Smith, A.M. Gurnell and G.R. McGregor (2000). An approach to
425 hydrograph classification. *Hydrological Processes*, 14, 317-338.
- 426 Herschy, R.W., 1995. Streamflow measurement. CRC Press.
- 427 Hodgkins, R., R. Cooper, M. Tranter and J. Wadham (2013). Drainage system development in
428 consecutive melt seasons at a polythermal, Arctic glacier, evaluated by flow recession
429 analysis and linear reservoir simulation. *Water Resources Research*, 49, 4230-4243.
- 430 Hudson, R. and J. Fraser (2005). The mass balance (or dry injection) method. *Streamline*
431 *Watershed Management Bulletin*, 9, 6-12.
- 432 Immerzeel, W.W. and M.F.P. Bierkens (2012). Asia's water balance. *Nature Geoscience*, 5, 841-
433 842.
- 434 Immerzeel, W.W., L.P.H. Van Beek and M.F.P. Bierkens (2010) Climate change will affect the
435 Asian water towers. *Science*, 328, 1382–1385.
- 436 Immerzeel, W.W., L.P.H. Van Beek, M. Konz, A.B. Shrestha and M.F.P. Bierkens (2012).
437 Hydrological response to climate change in a glacierized catchment in the Himalayas.
438 *Climatic Change*, 110, 721-736..
- 439 Jacobsen, D., A.M. Milner, L.E. Brown and O. Dangles (2012). Biodiversity under threat in
440 glacier-fed river systems. *Nature Climate Change*, 2, 361-364.

- 441 Jobard, S. and M. Dzikowski (2006). Evolution of glacial flow and drainage during the ablation
442 season. *Journal of Hydrology*, 330, 663-671.
- 443 Kääh, A., E. Berthier, C. Nuth, J. Gardelle and Y. Arnaud (2012) Contrasting patterns of early
444 twenty-first-century glacier mass change in the Himalayas. *Nature*, 488, 495-498.
- 445 King, O., D.J. Quincey, J.L. Carrivick and A.V. Rowan (2017). Spatial variability in mass loss of
446 glaciers in the Everest region, central Himalayas, between 2000 and 2015. *The
447 Cryosphere*, 11, 407-426.
- 448 Kirkbride, M.P. (1993). The temporal significance of transitions from melting to calving termini
449 at glaciers in the central Southern Alps of New Zealand. *The Holocene*, 3, 232-240.
- 450 Lang, H. (1973). Variations in the relation between glacier discharge and meteorological
451 elements. *IAHS Publication*, 95, 85-96.
- 452 Lutz, A. F., W.W. Immerzeel, A.B. Shrestha and M.F.P. Bierkens (2014). Consistent increase in
453 High Asia's runoff due to increasing glacier melt and precipitation. *Nature Climate
454 Change*, 4, 587-592.
- 455 McCarthy, M., H. Pritchard, I. Willis and E. King (2017). Ground-penetrating radar
456 measurements of debris thickness on Lirung Glacier, Nepal. *Journal of Glaciology*, 63,
457 543-555.
- 458 Mae, S., H. Wushiki, Y. Ageta and K. Higuchi (1975). Thermal drilling and temperature
459 measurements in Khumbu Glacier, Nepal Himalayas. *Seppyo*, 37, 161-169.
- 460 Mertes, J.R., S.S. Thompson, A.D. Booth, J.D. Gulley and D.I. Benn (2017). A conceptual
461 model of supra- glacial lake formation on debris- covered glaciers based on GPR facies
462 analysis. *Earth Surface Processes and Landforms*, 42, 903-914.
- 463 Miles, E.S., F. Pellicciotti, I.C. Willis, J.F. Steiner, P. Buri and N.S. Arnold (2016). Refined
464 energy-balance modelling of a supraglacial pond, Langtang Khola, Nepal. *Annals of
465 Glaciology*, 57, 29-40.
- 466 Miles, E.S., I.C. Willis, N.S. Arnold, J. Steiner and F. Pellicciotti (2017a). Spatial, seasonal and
467 interannual variability of supraglacial ponds in the Langtang Valley of Nepal, 1999–
468 2013. *Journal of Glaciology*, 63, 88-105.
- 469 Miles, E.S., J. Steiner, I. Willis, P. Buri, W.W. Immerzeel, A. Chesnokova, and F. Pellicciotti
470 (2017b). Pond Dynamics and Supraglacial-Englacial Connectivity on Debris-Covered
471 Lirung Glacier, Nepal. *Frontiers in Earth Science*, 5, 69.
- 472 Montaldo, N., M. Mancini and R. Rosso (2004). Flood hydrograph attenuation induced by a
473 reservoir system: analysis with a distributed rainfall-runoff model. *Hydrological
474 Processes*, 18, 545-563.
- 475 Muir, D.L., M. Hayashi and A.F. McClymont (2011). Hydrological storage and transmission
476 characteristics of an alpine talus. *Hydrological Processes*, 25, 2954-2966.
- 477 Narama, C., M. Daiyrov, T. Tadono, M. Yamamoto, A. Kääh, R. Morita and J. Ukita (2017).
478 Seasonal drainage of supraglacial lakes on debris-covered glaciers in the Tien Shan
479 Mountains, Central Asia. *Geomorphology*, 286, 133-142.

- 480 Nuimura, T., K. Fujita, K. Fukui, K. Asahi, R. Aryal and Y. Ageta (2011). Temporal changes in
481 elevation of the debris-covered ablation area of Khumbu Glacier in the Nepal Himalaya
482 since 1978. *Arctic, Antarctic, and Alpine Research*, 43, 246-255.
- 483 Østrem, G. (1959). Ice melting under a thin layer of moraine, and the existence of ice cores in
484 moraine ridges. *Geografiska Annaler*, 41, 228-230.
- 485 Parriaux, A., and G.F. Nicoud (1990). Hydrological behaviour of glacial deposits in mountainous
486 areas. *IAHS Publication* 190, 291-312.
- 487 Pritchard, H.D., 2017. Asia's glaciers are a regionally important buffer against
488 drought. *Nature*, 545(7653), 169-174.
- 489 Quincey, D.J., S.D. Richardson, A. Luckman, R.M. Lucas, J.M. Reynolds, M.J. Hambrey and
490 N.F. Glasser (2007). Early recognition of glacial lake hazards in the Himalaya using
491 remote sensing datasets. *Global and Planetary Change*, 56, 137-152.
- 492 Ragetti, S., F. Pellicciotti, W.W. Immerzeel, E.S. Miles, L. Petersen, M. Heynen, J.M. Shea, D.
493 Stumm, S. Joshi and A. Shrestha (2015). Unraveling the hydrology of a Himalayan
494 catchment through integration of high resolution in situ data and remote sensing with an
495 advanced simulation model. *Advances in Water Resources*, 78, 94-111.
- 496 Rantz, S.E., and others (1982). Measurement and computation of streamflow: Volume 2.
497 Computation of discharge. USGS Water Supply Paper 2175. USGPO, 285-631.
- 498 Reynolds, J.M. (2000). On the formation of supraglacial lakes on debris-covered glaciers. *IAHS*
499 *Publication*, 264, 153-164.
- 500 Richards, K., M. Sharp, N. Arnold, A. Gurnell, M. Clark, M. Tranter, P. Nienow, G. Brown, I.
501 Willis and W. Lawson (1996). An integrated approach to modelling hydrology and water
502 quality in glacierized catchments. *Hydrological Processes*, 10, 479-508.
- 503 Rowan, A.V., D.L. Egholm, D.J. Quincey and N.F. Glasser (2015). Modelling the feedbacks
504 between mass balance, ice flow and debris transport to predict the response to climate
505 change of debris-covered glaciers in the Himalaya, *Earth and Planetary Science Letters*,
506 430, 427-438.
- 507 Sakai, A., K. Fujita, T. Aoki, K. Asahi, and M. Nakawo (1997). Water discharge from the Lirung
508 Glacier in Langtang Valley, Nepal Himalayas, 1996. *Bulletin of Glacier Research* 15, 79-
509 83.
- 510 Sakai, A., M. Nakawo and K. Fujita (2002). Distribution characteristics and energy balance of
511 ice cliffs on debris-covered glaciers, Nepal Himalaya. *Arctic, Antarctic, and Alpine*
512 *Research*, 34, 12-19.
- 513 Sakai, A., N. Takeuchi, K. Fujita and M. Nakawo (2000). Role of supraglacial ponds in the
514 ablation process of a debris-covered glacier in the Nepal Himalayas. *IAHS Publication*,
515 264, 119-132.
- 516 Salerno, F., M. Rogora, R. Balestrini, A. Lami, G.A. Tartari, S. Thakuri, D. Godone, M. Freppaz
517 and G. Tartari (2016). Glacier melting increases the solute concentrations of Himalayan
518 glacial lakes. *Environmental Science & Technology*, 50, 9150-9160.

- 519 Salerno, F., S. Thakuri, G. Tartari, T. Nuimura, S. Sunako, A. Sakai, K. Fujita. 2017. Debris-
520 covered glacier anomaly? Morphological factors controlling changes in the mass balance,
521 surface area, terminus position, and snow line altitude of Himalayan glaciers. *Earth and*
522 *Planetary Science Letters*, 471, 19-31.
- 523 Scherler, D., B. Bookhagen and M.R. Strecker (2011). Spatially variable response of Himalayan
524 glaciers to climate change affected by debris cover. *Nature Geoscience*, 4, 156-159.
- 525 Schmid, M.O., P. Baral, S. Gruber, S. Shahi, T. Shrestha, D. Stumm and P. Wester (2015).
526 Assessment of permafrost distribution maps in the Hindu Kush Himalayan region using
527 rock glaciers mapped in Google Earth. *The Cryosphere*, 9, 2089-2099.
- 528 Shea, J.M., W.W. Immerzeel, P. Wagnon, C. Vincent and S. Bajracharya (2015a). Modelling
529 glacier change in the Everest region, Nepal Himalaya. *The Cryosphere*, 9, 1105-1128.
- 530 Shea J.M., P. Wagnon, W.W. Immerzeel, R. Biron, F. Brun and F. Pellicciotti. (2015b). A
531 comparative high-altitude meteorological analysis from three catchments in the Nepalese
532 Himalaya, *International Journal of Water Resources Development*, 31, 174-200.
- 533 Sherpa, S.F., P. Wagnon, F. Brun, E. Berthier, C. Vincent, Y. Lejeune, Y. Arnaud, R.B.
534 Kayastha and A. Sinisolo (2017). Contrasted surface mass balances of debris-free
535 glaciers observed between the southern and the inner parts of the Everest region (2007–
536 15). *Journal of Glaciology*, XX, 1-15. doi: 10.1017/jog.2017.30
- 537 Soncini, A., D. Bocchiola, G. Confortola, U. Minora, E. Vuillermoz, F. Salerno, G. Viviano, D.
538 Shrestha, A. Senese, C. Smiraglia, and G. Diolaiuti (2016). Future hydrological regimes
539 and glacier cover in the Everest region: The case study of the upper Dudh Koshi basin.
540 *Science of the Total Environment*, 565, 1084-1101. doi: 10.1016/j.scitotenv.2016.05.138
- 541 Steiner, J.F. and F. Pellicciotti (2016). Variability of air temperature over a debris-covered
542 glacier in the Nepalese Himalaya. *Annals of Glaciology*, 57, 295-307.
- 543 Swift, D.A., P.W. Nienow, T.B. Hoey and D.W. Mair (2005). Seasonal evolution of runoff from
544 Haut Glacier d'Arolla, Switzerland and implications for glacial geomorphic processes.
545 *Journal of Hydrology*, 309,133-148.
- 546 Takeuchi, N., A. Sakai, K. Shiro, K. Fujita and N. Masayoshi (2012). Variation in suspended
547 sediment concentration of supraglacial lakes on debris-covered area of the Lirung Glacier
548 in the Nepal Himalayas. *Global Environmental Reseach*, 16, 95-104.
- 549 Thakuri, S., F. Salerno, C. Smiraglia, T. Bolch, C. D'Agata, G. Viviano and G. Tartari (2014).
550 Tracing glacier changes since the 1960s on the south slope of Mt. Everest (central
551 Southern Himalaya) using optical satellite imagery. *The Cryosphere*, 8, 1297-1315.
- 552 Thayyen, R.J., J.T. Gergan and D.P. Dobhal (2005). Monsoonal control on glacier discharge and
553 hydrograph characteristics, a case study of Dokriani Glacier, Garhwal Himalaya, India.
554 *Journal of Hydrology*, 306, 37-49.
- 555 Thompson, S., D.I. Benn, J. Mertes and A. Luckman (2016). Stagnation and mass loss on a
556 Himalayan debris-covered glacier: processes, patterns and rates. *Journal of Glaciology*,
557 62, 67-485.

- 558 Verbunt, M., J. Gurtz, K. Jasper, H. Lang, P. Warmerdam, and M. Zappa (2003). The
559 hydrological role of snow and glaciers in alpine river basins and their distributed
560 modeling. *Journal of Hydrology*, 282(1), 36-55.
- 561 Vincent, C., P. Wagnon, J.M. Shea, W.W. Immerzeel, P. Kraaijenbrink, D. Shrestha, A. Soruco,
562 Y. Arnaud, F. Brun, E. Berthier, S.F. Sherpa (2016). Reduced melt on debris-covered
563 glaciers: investigations from Changri Nup Glacier, Nepal. *The Cryosphere*, 10, 1845-
564 1858.
- 565 Watson, S. C., D.J. Quincey, J.L. Carrivick and M.W. Smith (2016). The dynamics of
566 supraglacial water storage in the Everest region, central Himalaya. *Global and Planetary*
567 *Change*, 142, 14-27.
- 568 Watson, C.S., D.J. Quincey, J.L. Carrivick, M.W. Smith, A.V. Rowan and R. Richardson
569 (2017a). Heterogeneous water storage and thermal regime of supraglacial ponds on
570 debris-covered glaciers. *Earth Surface Processes and Landforms* (early view) doi:
571 10.1002/esp.4236.
- 572 Watson, C.S., D.J. Quincey, J.L. Carrivick and M.W. Smith (2017b). Ice cliff dynamics in the
573 Everest region of the Central Himalaya. *Geomorphology*, 278, 238-251.
- 574 Wessels, R.L., J.S. Kargel and H.H. Kieffer (2002). ASTER measurement of supraglacial lakes
575 in the Mount Everest region of the Himalaya. *Annals of Glaciology*, 34, 399-40.
- 576 Woo, M.K. and P. Steer (1983). Slope hydrology as influenced by thawing of the active layer,
577 Resolute, NWT. *Canadian Journal of Earth Sciences*, 20, 978-986.
- 578 Woo, M.K. and Z. Xia (1995). Suprapermafrost groundwater seepage in gravelly terrain,
579 Resolute, NWT, Canada. *Permafrost and Periglacial Processes*, 6(1), 57-72.
- 580 Xu, J., R.E. Grumbine, A. Shrestha, M. Eriksson, X. Yang, Y. Wang and A. Wilkes (2009). The
581 melting Himalayas: cascading effects of climate change on water, biodiversity, and
582 livelihoods. *Conservation Biology*, 23, 520-530.